PERFORMANCE OF THE OPTIMAL NONLINEAR DETECTOR/TRACKER IN CLUTTER

Marcelo G. S. Bruno and José M. F. Moura

Department of Electrical and Computer Engineering
Carnegie Mellon University, Pittsburgh, PA, 15213
ph: (412)268-6341; fax: (412)268-3890; email: moura@ece.cmu.edu

ABSTRACT

We propose in this paper an optimal nonlinear Bayesian algorithm for joint detection and tracking of targets that move randomly in cluttered environments. We review the derivation of the optimal Bayesian detector/tracker and present Monte Carlo simulations that benchmark the detection and tracking performances in both spatially correlated and non-Gaussian clutter.

1. INTRODUCTION

The problem we consider in this paper is to detect and track moving targets using noisy sensor measurements. The traditional approach to this problem involves the separation of the detection and tracking tasks [1]. In this paper, we present an alternative approach that integrates the detection problem into the same framework in which the tracking problem is solved.

We apply nonlinear stochastic filtering to design the optimal joint tracker/detector. We restrict our discussion to rigid bodies with translational motion such that the problem of tracking a target reduces to the tracking of its centroid position. We use a Bayesian strategy to compute recursively the posterior probabilities of all possible centroid positions at the nth sensor scan conditioned on the present and all past observations. An additional state representing the absence of the target is used to build an integrated framework for detection and tracking.

Section 2 reviews briefly the models for target signature, target motion, and clutter statistics [2] that underly our integrated framework for detection and tracking. Three classes of clutter models are assumed: white Gaussian clutter, spatially correlated Gauss-Markov clutter [3], and white non-Gaussian clutter [4] with heavytail envelope statistics (K and Weibull clutter). In section 3, we derive the optimal nonlinear detector/tracker. Section 4 presents receiver operating characteristic (ROC)

curves that quantify the detection performance of the algorithm for the different clutter models. Section 5 examines tracking performance and quantifies the performance gain of the nonlinear Bayesian tracker over other schemes commonly found in the literature such as maximum likelihood (ML) trackers and linearized Kalman-Bucy filters (KBfs). Finally, section 6 concludes the paper.

2. THE MODEL

We review briefly in this section the models for target signature, target motion, and clutter statistics. For simplicity, we restrict ourselves to a scenario with one-dimensional (1D) surveillance spaces (e.g., radial motion with constant azimuth and elevation) and a single target per sensor scan. The extension of the models to two-dimensional (2D) environments (targets that move randomly in a plane) and to a multitarget scenario is detailed in [2].

Sensor Model

The sensor scans a bounded surveillance region which, given the sensor's finite resolution, is discretized by a uniform finite discrete lattice. Assuming a 1D surveillance region, the sensor lattice is an interval of the real line given by $\mathcal{L} = \{l : 1 \leq l \leq L\}$ where L is the number of resolution cells.

We introduce now the random variable z_n that represents the target centroid position (range) in the sensor lattice during the nth sensor scan. In order to account for the situations when targets move in and out of the sensor range and in order to account for the possibility of absence of target, we define z_n on an *augmented lattice* [2]. The augmented lattice includes possible centroid positions that actually lie outside the sensor range but, for which, due to the physical dimensions of the target, at least one pixel of the target may be still present in the sensor image. The augmented lattice also includes an additional artificial state that mathematically represents the absence of a target. In the 1D case, the augmented lattice is then

$\tilde{\mathcal{L}} = \{l: -l_s + 1 \leq l \leq L + l_i + 1\}$, where $(l_i + l_s + 1)$ is the maximum length of the 1D noise free image of a possible target and $z_n = L + l_i + 1$ means that no target is present at instant n.

Motion Model

The motion dynamics of a target in the corresponding augmented lattice $\tilde{\mathcal{L}}$ is specified by a *transition probability matrix*, $\mathbf{T}$, whose general element $T(k,r)$ is

$$T(k,r) = \text{Prob}(z_n = k - l_s \mid z_{n-1} = r - l_s) \quad (1)$$

where $1 \leq k, r \leq L + l_i + l_s + 1$.

Observations

The observations at the nth sensor scan, assuming a 1D surveillance region and a single target per frame, are collected in the L-dimensional column vector

$$\mathbf{y}_n = \mathbf{f}(z_n) + \mathbf{v}_n \quad (2)$$

where $\mathbf{v}_n$ is the background clutter and $\mathbf{f}(z_n)$ is an appropriate nonlinear target model.

We assume the following models for the statistics of the clutter: (1) white Gaussian noise; (2) spatially correlated *noncausal* Gauss-Markov random sequence (GMrseq); (3) uncorrelated non-Gaussian complex clutter with K-envelope statistics; (4) uncorrelated non-Gaussian complex clutter with Weibull envelope statistics. Details on these models and on the simulation of the corresponding clutter samples are found in [2, 3, 4]. The target model, on the other hand, maps a centroid position z_n, for all states different from the absent state, into a noise-free image. The noise-free target image is characterized by a set of signature parameters which, in general, are factored into a deterministic shape component and a possibly unknown/random pixel intensity component. When $z_n = L + l_i + 1$, i.e., when there is no target present during the nth sensor scan, the target model maps z_n into a null image. The complete target model is detailed in [2].

3. OPTIMAL DETECTOR/TRACKER

We assume for simplicity that at each sensor scan only one single target may be present at the surveillance space. The extension of the detection/tracking algorithm to a multitarget scenario is found in [2]. Given the observations $\mathbf{y}_0^n = [\mathbf{y}_0 \, \mathbf{y}_1 \ldots \mathbf{y}_n]$, from instant 0 up to instant n, we want, at each instant n, to determine whether a target is present or not (detection) and, if the target is declared present, to estimate its position (range) in the surveillance space (tracking).

Optimal Bayesian Detector/Tracker

The optimal statistical solution for the joint detection/tracking problem follows a Bayesian strategy.

From a Bayesian point of view, it suffices to compute at each instant n, the posterior probabilities $P(z_n \mid \mathbf{y}_0^n)$, for all possible values of the random variable z_n, including the absent state. The formal solution is divided into two steps:

Filtering Step: From Bayes' law,

$$P(z_n \mid \mathbf{y}_0^n) = C_n p(\mathbf{y}_n \mid z_n) P(z_n \mid \mathbf{y}_0^{n-1}) \quad (3)$$

where C_n is a normalization constant.

Prediction Step: From the total probability theorem

$$P(z_n \mid \mathbf{y}_0^{n-1}) = \sum_{z_{n-1}} P(z_n \mid z_{n-1}) P(z_{n-1} \mid \mathbf{y}_0^{n-1}) \, . \quad (4)$$

We now detail the minimum probability of error detector and the optimal MAP tracker.

Detector: Let H_0 denote the hypothesis that no target is present at instant n and H_1 denote the hypothesis that a target is present during the nth sensor scan. Given $P(z_n \mid \mathbf{y}_0^n)$, compute the posterior probabilities of the detection hypothesis $H_j, j = 0, 1$. The minimum probability of error Bayes detector follows the decision rule

$$P(H_0 \mid \mathbf{y}_0^n) \underset{H_1}{\overset{H_0}{\gtrless}} P(H_1 \mid \mathbf{y}_0^n) \, . \quad (5)$$

Tracker: If hypothesis H_1 is declared true, compute the conditional probability vector $\mathbf{\Pi}_{n|n}^i$ such that

$$\Pi_{n|n}^i(z_n) = P(z_n \mid H_1, \mathbf{y}_0^n) = \frac{P(z_n, H_1 \mid \mathbf{y}_0^n)}{P(H_1 \mid \mathbf{y}_0^n)} \, . \quad (6)$$

The MAP Bayes tracker looks for the maximum of $\mathbf{\Pi}_{n|n}^i$ to estimate the position of target.

4. DETECTION PERFORMANCE

We examine in this section the detection performance of the optimal nonlinear detector/tracker. If we vary the threshold in (5) over a wide range, the detection algorithm operates as a *Neyman-Pearson* detector where a fixed value of probability of false alarm is associated with each value of the threshold. The performance of the detector is assessed then by a ROC curve where the different combinations of probabilities of false alarm (P_{fa}) and probability of detection (P_d) are plotted for a given level of peak signal-to-noise ratio (PSNR).

The experimental ROC curves presented in this section are obtained through *Monte Carlo* simulations. For simplicity, the simulations use a succession of single targets with time-invariant, deterministic, unit signature. The targets move in a sensor resolution grid of

$L = 64$ cells with a mean drift of 2 cells/scan. There is a fluctuation probability of one cell around the mean displacement equal to 0.4. As one target disappears from the surveillance space, there is a 20 % probability of a new target reappearing at any arbitrary position in the grid $\mathcal{L} = \{l{:}1 \leq l \leq L\}$. For each threshold value, we use 10,000 sensor scans to compute the corresponding false alarm and detection statistics.

Gaussian Clutter: We present initially the detection statistics under Gaussian clutter. Figure 1 shows the probability of detection versus probability of false alarm for spatially uncorrelated (white) Gaussian clutter with levels of PSNR equal to 10, 6, and 3 dB from top to bottom. Figure 1(b) plots the detection statistics for spatially *correlated* clutter modeled by a first-order *noncausal* GMrseq with correlation parameter $\alpha_1 = 0.24$. In figure 1(b), the levels of PSNR from top to bottom are 8, 6, and 3 dB respectively. We notice

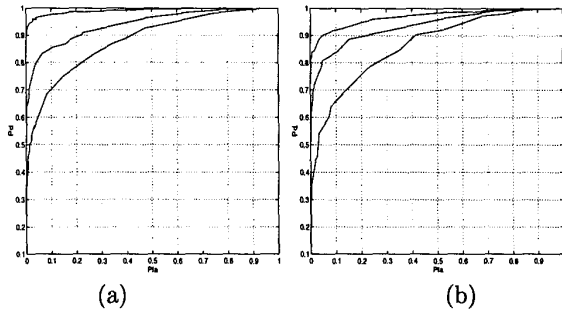(a)   (b)

Figure 1: ROC curves for Gaussian clutter: (a) white, (b) correlated GMRseq, $\alpha_1 = 0.24$

from figures 1(a) and (b) that, as the PSNR increases the ROC curves tend to a "step-like" shape, i.e., for low levels of false alarm, we observe correspondingly much higher levels of detection. The performance deteriorates as expected as we increase the power of the background noise. However, even in adverse scenarios such as the situation when PSNR = 3 dB, the ROC curves still remain significantly above the 45$^{\underline{o}}$ line. This behavior highlights good detection performance even in very noisy environments.

In order to evaluate the effect of the degree of clutter spatial correlation on the detection performance, we show in figure 2 the superposition of the ROC curves obtained with white Gaussian (spatially uncorrelated) clutter, correlated clutter with $\alpha_1 = 0.24$ (low spatial correlation), and correlated clutter with $\alpha_1 = 0.49$ (high spatial correlation). The peak signal-to-noise ratios from top to bottom are 6 and 3 dB respectively. Figure 2 indicates that, for these two levels of PSNR, there is little perceptible difference, within the margin

of error in the experiment, between the detection performances under uncorrelated, weakly correlated, and strongly correlated clutter. That suggests a possible robustness of the optimal detector with respect to clutter correlation.
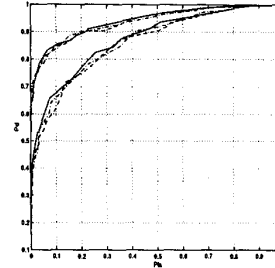

Figure 2: Comparison of detection performances for white Gaussian clutter (solid), weakly correlated GMrseq clutter (dotted), and highly correlated GMRseq clutter (dashdotted); top to bottom: PSNR=6 dB and PSNR= 3 dB

Non-Gaussian Clutter: To evaluate the detection performance for non-Gaussian clutter, we ran Monte Carlo simulations with a succession of single pointwise targets moving in uncorrelated complex clutter with K and Weibull envelope statistics. The motion parameters are the same as in the Gaussian simulation, except that, in the case of complex clutter, a drift of d resolutions cells/scan corresponds to a drift of $2d$ in the double-sized sensor image. The probabilities of detection and false alarm for each value of threshold are obtained from statistics collected from 10000 sensor scans, where each scan corresponds to 64 resolution cells or 128 complex quadrature returns. We generate 8,064 samples of background clutter every 63 scans.

Figure 3(a) and (b) show the experimental ROC curves for K and Weibull clutter respectively, with PSNR equal to 6 and 3 dB from top to bottom. We note that even in these situations of low PSNR per scan and adverse heavy-tail clutter, the ROC curve still remain significantly above the 45$^{\underline{o}}$ degree line.

5. TRACKING PERFORMANCE

In this section, we compare the performance of the optimal nonlinear MAP tracking algorithm introduced in section 3 with the performance of other suboptimal trackers found in the literature: the memoryless maximum likelihood (ML) tracker and the linearized Kalman-Bucy tracker [2].

Figure 4(a) illustrates the tracking results for the three schemes in correlated Gauss-Markov clutter with
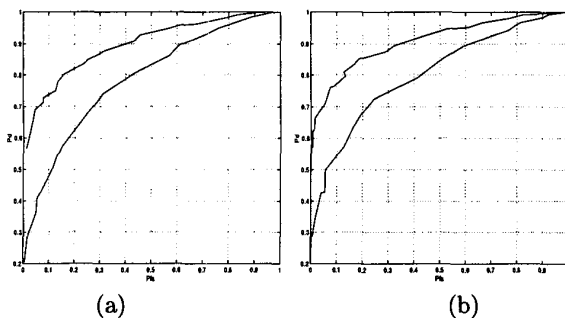
Figure 3: ROC curves for non-Gaussian clutter: (a) K envelope, (b) Weibull envelope; top to bottom, PSNR=6 and 3 dB

correlation parameter 0.24. The simulated trajectory corresponds to a unit signature pointwise target that moves in a 300 resolution cells sensor grid with a mean drift of 2 cells/frame and a fluctuation probability of one cell around the mean displacement equal to 20 %. The PSNR per scan is 10 dB. The solid line is the real trajectory. The dashed line corresponds to the ML track and the dashdotted line shows the output of the linearized Kalman-Bucy tracker. The tracking results for the optimal nonlinear tracker proposed in this paper are indicated by the symbol '+'. Figure 4(a) illustrates the poor performance of the ML tracker in low PSNR environments. When the output of the ML tracker is corrected by the linearized Kalman-Bucy filter (KBf), the tracking performance improves due to the inertia in the prediction step of the KBf. The trajectory estimated by the optimal nonlinear tracker overlap, on the other hand, the true trajectory evidentiating superior performance over the linearized KBf.
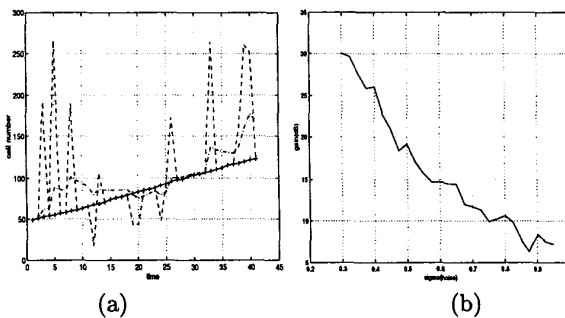

Figure 4: (a) Tracking examples with correlated clutter for ML tracker (dotted), Kalman-Bucy tracker (dash-dotted), and nonlinear tracker (+), PSNR=10 dB; (b) Performance gain of the nonlinear tracker over the KBf tracker for correlated clutter

In order to quantify the gain in tracking performance provided by the optimal nonlinear tracker, we ran Monte Carlo simulations to estimate the variance of the tracking error for each of the three tracking schemes. The variance was computed by an average over 6500 sensor scans with 300 resolution cells per scan. The initial tracking error is set to zero for the 3 trackers. The measurement noise variance in the linearized KBf is adaptively adjusted to follow the estimated error variance of the ML tracker for each value of PSNR per scan. Figure 4(b) shows the gain $G = 20 \log \sigma_{kbf}/\sigma_{nl}$ when the standard deviation of the background noise is varied from $\sigma = 0.3$ (PSNR=10 dB) to $\sigma = 0.95$ (PSNR= 0.5 dB). We observe that the performance gain over the linearized KBf ranges from 30 dB for PSNR=10 dB to 7 dB for PSNR close to 0 dB.

6. CONCLUSIONS

We derived in this paper an optimal nonlinear joint detector/tracker for targets that move randomly on a finite discrete grid. We presented Monte Carlo simulations that quantify the detection and tracking performances in scenarios with spatially correlated Gaussian clutter and uncorrelated non-Gaussian clutter with heavy-tail envelope statistics (K and Weibull clutter). These results benchmark the performance gains to be had by any suboptimal detection/tracking algorithm.

7. REFERENCES

[1] Y. Bar-Shalom and X. Li.*Multitarget-Multisensor Tracking: Principles and Techniques*. YBS, Storrs, CT, 1995.

[2] M. G. S. Bruno. *Joint Detection and Tracking of Moving Targets in Clutter*. Ph.D. Thesis, ECE Department, Carnegie Mellon University, May 6, 1998.

[3] J. M. F. Moura and N. Balram. Recursive Structure of Noncausal Gauss Markov Random Fields. *IEEE Transactions on Information Theory* IT-38(2): 334-354, March 1992.

[4] M. Rangaswamy, D. Weiner and A. Öztürk. Computer generation of correlated non-Gaussian radar clutter. *IEEE Transactions on Aerospace and Electronic Systems*. Vol 31, No. 1, pp 106-116, January 1995.